

Note: The originally published ESI document for DOI: 10.1039/c9tc01178a was replaced with this version on 14th February 2020

Room temperature Discotic Liquid Crystalline Triphenylene-Pentaalkynylbenzene dyads as an emitter in blue OLEDs and their Charge transfer complexes with ambipolar charge transport behaviour

Indu Bala,^a Wan-Yun Yang,^b Santosh Prasad Gupta,^c Joydip De,^a Rohit Ashok Kumar Yadav,^b Dharmendra Pratap Singh,^d Deepak Kumar Dubey,^b Jwo-Huei Jou^b, Redouane Douali^d and Santanu Kumar Pal^{*a}

^aIndian Institute of Science Education and Research (IISER) Mohali, Sector-81, SAS Nagar, Mohali 140306, India.
E-mail: skpal@iisermohali.ac.in

^bDepartment of Materials Science and Engineering, National Tsing Hua University, Hsinchu 30013, Taiwan

^cDepartment of Physics, Patna University, Patna- 800005

^dUnité de Dynamique et Structure des Matériaux Moléculaires (UDSMM), Université du Littoral Côte d'Opale (ULCO), 50 Rue Ferdinand Buisson, 62228, Calais, France

Table of contents		
S. No.	Contents	Page No.
1.	Experimental Section	S2-S4
2.	Synthetic details of intermediates and final compounds	S4-S8
3.	Spectral characterization data (¹ H and ¹³ C)	S8-S14
4.	FT-IR spectral data	S14
5.	DSC thermogram	S15
6.	X-Ray data	S15-S20
7.	Absorption and Emission studies	S20-S21
8.	Quantum Yield Calculation	S22-S23
9.	Fluorescence decay measurements	S24
10.	References	S24

1. Experimental Section

1.1 Materials and reagents: The chemicals and solvents used during the synthesis and studies of the materials described in the manuscript were all of AR quality and used without any prior purification. Pentabromophenol, potassium carbonate (K_2CO_3), dibromohexane, dibromooctane, dibromodecane, 4-pentyl phenylacetylene, copper iodide (CuI), bis(triphenylphosphine) palladium(II) dichloride ($Pd(PPh_3)_2Cl_2$), triphenylphosphine (PPh_3), triethylamine (Et_3N), Potassium hydroxide (KOH), tetraoctylammoniumbromide (TOAB) were all purchased from Sigma-Aldrich (Bangalore, India). Potassium iodide (KI) and hydrochloric acid (HCl) were purchased from Merck. Column chromatographic separations were performed on silica gel (60-120) and neutral alumina gel. Thin layer chromatography (TLC) was performed on alumina sheets pre-coated with silica gel (Merck, Kieselgel 60, F254).

Indium-tin oxide (ITO) coated glass substrates were purchased from the Luminescence Technology Corporation, Taiwan. The sublimated grade materials Poly(3,4-ethylenedioxythiophene)-poly(styrenesulfonate) (PEDOT:PSS) and lithium fluoride (LiF) were purchased from Sigma-Aldrich Inc., USA. The hosts 4,4'-Bis(N-carbazolyl)-1,1'-biphenyl (CBP), 2,7-Bis(carbazol-9-yl)-9,9-spirobifluorene (Spiro-2CBP), Tris(4-carbazoyl-9-ylphenyl)amine (TCTA), and electron transport material 2,2',2''-(1,3,5-Benzinetriyl)-tris(1-phenyl-1-H-benzimidazole) (TPBi) were purchased from the Luminescence Technology Corporation, Taiwan. Aluminum (Al) ingots (99.999%) were purchased from Showa Chemical Co. Ltd., Japan.

1.2 Instrumentation

The details of instrumentations and other studies have been provided as reported in our previous manuscript.¹

1.2.1 Structural characterization¹: “¹H NMR and ¹³C NMR (Bruker Biospin Switzerland Avance-iii 400 MHz and 100 MHz spectrometers, respectively), UV-VIS-NIR spectrophotometer (Agilent Technologies UV-Vis-NIR Spectrophotometer). NMR spectra were recorded using deuterated chloroform ($CDCl_3$) as solvent and tetramethylsilane (TMS) as an internal standard.”

1.2.2 Polarised Optical Microscopy¹: “Textural observations of the mesophase were performed with Nikon Eclipse LV100POL polarising microscope provided with a Linkam heating stage (LTS 420). All images were captured using a Q-imaging camera.”

1.2.3 DSC Study¹: “The transition temperatures and associated enthalpy values were determined using a differential scanning calorimeter (Perkin Elmer DSC 8000 coupled to a controlled liquid nitrogen accessory (CLN 2)) which was operated at a scanning rate of 10 °C min⁻¹ both on heating and cooling.”

1.2.4 X-ray diffraction studies¹: “X-ray diffraction (XRD) was carried out using Cu K α ($\lambda=1.54$ Å) radiation from a source (GeniX 3D, Xenocs) operating at 50 kV and 0.6 mA. The diffraction patterns were collected on a two module Pilatus detector.”

1.2.5 Photophysical studies¹: “Fluorescence emission spectra and steady state anisotropy experiments were performed on Horiba Scientific Fluoromax spectrofluorometer 4. Time resolved lifetime measurements were done on time correlated single photon counter from Horiba Jobin Yvon.”

1.2.6 Electrochemical studies¹: “Cyclic Voltammetry experiments were performed on CH Instruments, electrochemical workstation.”

1.2.7 Electron density map¹: The details have reported elsewhere.¹ “The electron density $\rho(x,y)$ of a liquid crystal is linked to its structure factor $F(hk)$ by inverse Fourier transformation:

$$\rho(x,y) = \sum F(hk) e^{2\pi i(hx+ky)}$$

In this formula (hk) are the Miller Indices and x, y the fractional coordinates in the unit cell. To calculate the electron density, the complex structure factor (hk) has to be written as the product of the phase $\Phi(hk)$ and the modulus $|F(hk)|$ which is proportional to the square root of the intensity $I(hk)$ of the observed reflection

$$F(hk) = |F(hk)|e^{i\Phi(hk)} = \sqrt{I(hk)}e^{i\Phi(hk)}$$

While the intensity $I(hk)$ can be easily obtained from the X-ray diffraction experiment, the only information that cannot be obtained directly from experiment is the phase $\Phi(hk)$ for each diffraction peak. However, this problem becomes easily tractable when the structure under study is centro-symmetric, that if $\rho(x,y)=\rho(-x,-y)$, $F(hk)$ can only be real hence, $\Phi(hk)$ can only be 0 or π . For non-centro-symmetric groups, the phase may take every value between 0 and 2π . Since the columnar phase observed in these compound assemblies are centro-symmetric and have only limited number of diffraction peaks, it is possible to reconstruct electron density

maps of all possible phase combinations. The “correct” map is subsequently chosen on the merit of the reconstructed maps and other physical and chemical knowledge of the system such as, chemical constituents and their sizes *etc.*”

2. Synthetic details

The compounds **2a-c** were prepared according to the procedure as reported in earlier reports.^{1,2}

2.1 General procedure for the synthesis of the compound 2a-c: In a round bottom flask (R.B), pentabromophenol (1 equiv.), potassium carbonate (5 equiv.) and alkyl bromide (5 equiv.) was refluxed in a 30 ml dry acetone for 12 hours. Potassium iodide was added in a catalytic amount. After completion of the reaction, the acetone was evaporated and then extracted with DCM. The reaction mixture was purified in 100-120 silica gel by using hexane/EtOAc as an eluent.

The compounds **3a-c** were prepared according to the procedure as reported in previous reports.^{1,2}

2.2 General procedure for the synthesis of the compound 3a-c: The sonogshira of alkylated compound **2** (500 mg) was done by taking 30 ml of dry triethylamine in a round bottom flask which was degassed followed by the addition of Pd(PPh₃)₂Cl₂ (50 mg), CuI (50 mg) & PPh₃ (100 mg). The mixture was stirred for 15 minutes followed by the gradual addition of 4-pentylphenylacetylene. The reaction mixture was stirred at 100 °C for 24 h under nitrogen atmosphere & after cooling to room temperature it was poured into 30 ml of 5M HCl. After extracting the reaction mixture with DCM, the compound was purified in 230-400 silica gel by using hexane/EtOAc as an eluent.

The compounds **4a-c** were prepared according to the procedure as reported in previous reports.³

2.3 General procedure for the synthesis of the compound 4a-c: A mixture of compound **2** (1 equiv.) and NaN₃ (13 equiv.) in DMF (10 mL) was stirred at room temperature for 12 h. After addition of water, it was extracted with diethyl ether. The organic layer was dried with Na₂SO₄, and solvent was removed under reduced pressure. The compound was used without further purification.

The hexahexyloxytriphenylene **5** and monohydroxytriphenylene **6** were prepared as reported in several reports earlier.^{4,5} The compound **7** (**m=1** & **m=2**) were prepared as per reference no. 3.

2.4 General procedure for the synthesis of the compound 7 (m=1 & m=2, see Scheme 1 in main manuscript): To the mixture of compound **6** (1 equiv.) and K₂CO₃ (4 equiv.) in DMF (3 mL), the terminal alkyne (1-bromo-propyne, m=1 & 3-bromo-1-propyne, m=2) (16 equiv.) was added, and the mixture was stirred over 12 h at 50 °C. After removing the solvent, the residue was washed with water and extracted with diethylether. The organic layer was dried with Na₂SO₄, and the organic solvent was removed under vacuum. The crude product was purified by column chromatography with 60-120 silica gel by using hexane/ethyl acetate as an eluent to get the product as a white solid.

2.5 General procedure for the synthesis of the target compounds 8a-c & 9a-c: Compound **4** (1 equiv.) and **7** (m=1 & m=2) (1 equiv.) were dissolved in toluene (2 mL), then CuI (1.4 equiv.) and NEt₃ (0.24 equiv.) was added. The resulting mixture was stirred for 12 h at room temperature. Then toluene was removed under reduced pressure, and the residual solid was purified by column chromatography with 100-200 silica gel by using hexane/ethyl acetate as an eluent to obtain the product as a yellowish brown solid.

The NMR of only target compounds have been provided, the NMRs of the intermediates can be found in the corresponding cited references. The target compounds **8a-c** and **9a-c** were comprehensively characterized by ¹H NMR, ¹³C NMR, FT-IR, HRMS. The spectral details of the target compounds **8a-c** & **9a-c** ¹H NMR, ¹³C NMR, FT-IR, HRMS are detailed as below:

2.6 Spectral data details of the final compounds 8a-c and 9a-c:

Compound 8a:

FT-IR (cm⁻¹): 2955.50, 2929.29, 2857.60, 2208.29, 1741.7, 1616.47, 1513.31, 1466.87, 1434.80, 1379.78, 1346.81, 1262.10, 1168.74, 1085.9, 1043.22, 838.01, 726.72, 597.89, 551.11.

¹H NMR (400 MHz, CDCl₃, δ in ppm): δ 8.08 (s, 1H), δ 7.83 (s, 1H), δ 7.81 (s, 4H), δ 7.58 (s, 1H), δ 7.54-7.47 (m, 10H), δ 7.18-7.15 (m, 10H), δ 5.49 (s, 2H), 4.29-4.19 (m, 14H), 2.65-2.58 (m, 10H), 1.98-1.88 (m, 10H), 1.86-1.81 (m, 4H), 1.62-1.56 (m, 22H), 1.43-1.28 (m, 42H), 0.94-0.86 (m, 30H).

¹³C NMR (100 MHz, CDCl₃, δ in ppm): δ 160.11, 149.44, 149.26, 148.87, 147.83, 144.70, 144.19, 144.16, 143.87, 131.90, 131.78, 131.66, 128.94, 128.72, 128.67, 128.64, 124.28, 123.83, 123.61, 123.38, 123.27, 122.75, 120.78, 120.57, 120.54, 120.10, 108.95, 107.59, 107.21, 106.77, 106.49, 99.76, 99.41, 97.52, 87.15, 84.15, 74.26, 70.03, 69.92, 69.70, 64.15,

50.40, 36.12, 36.07, 32.07, 31.85, 31.82, 31.62, 31.60, 31.09, 30.31, 29.85, 29.59, 29.56, 29.48, 26.51, 26.00, 25.99, 25.91, 22.81, 22.68, 22.66, 14.58, 14.21, 14.19.

HRMS (MALDI) for $C_{128}H_{161}N_3O_7$ (M + H): calculated – 1854.2446; found- 1854.2546.

Compound 8b:

FT-IR (cm^{-1}): 2955.70, 2928.78, 2857.00, 2208.11, 1737.80, 1616.56, 1513.26, 1466.75, 1434.99, 1379.64, 1346.81, 1262.43, 1169.64, 1085.9, 1042.80, 838.12, 726.08, 593.98, 547.14.

1H NMR (400 MHz, $CDCl_3$, δ in ppm): δ 8.09 (s, 1H), δ 7.84 (s, 1H), δ 7.82 (s, 4H), δ 7.64 (s, 1H), δ 7.55-7.49 (m, 10H), δ 7.18-7.15 (m, 10H), δ 5.50 (s, 2H), 4.35-4.20 (m, 14H), 2.64-2.59 (m, 10H), 1.99-1.83 (m, 14H), 1.67-1.55 (m, 22H), 1.44-1.25 (m, 46H), 0.95-0.87 (m, 30H).

^{13}C NMR (100 MHz, $CDCl_3$, δ in ppm): δ 160.25, 149.44, 149.26, 148.91, 148.86, 147.86, 144.72, 144.17, 144.08, 143.85, 131.89, 131.77, 131.69, 128.91, 128.68, 128.64, 124.27, 124.24, 124.06, 123.83, 123.63, 123.38, 123.25, 122.73, 120.79, 120.63, 120.56, 120.14, 108.95, 107.61, 107.22, 106.48, 99.70, 99.46, 97.46, 87.17, 86.68, 84.22, 74.70, 70.03, 69.93, 69.71, 69.54, 69.34, 64.17, 50.54, 36.12, 31.84, 31.62, 31.60, 31.11, 31.08, 30.59, 30.37, 29.85, 29.58, 29.55, 29.48, 29.40, 29.04, 26.59, 26.34, 26.00, 22.82, 22.68, 14.21, 14.19.

HRMS (MALDI) for $C_{130}H_{165}N_3O_7$ (M + H): calculated – 1882.2759; found- 1882.2852.

Compound 8c:

FT-IR (cm^{-1}): 2959.70, 2928.61, 2856.84, 2210.10, 1733.90, 1616.08, 1512.89, 1468.40, 1434.65, 1379.77, 1262.10, 1170.59, 1085.90, 1041.72, 839.92, 802.90, 730.61, 597.89, 558.85.

1H NMR (400 MHz, $CDCl_3$, δ in ppm): δ 8.09 (s, 1H), δ 7.84 (s, 1H), δ 7.82 (s, 4H), δ 7.65 (s, 1H), δ 7.55-7.49 (m, 10H), δ 7.17-7.15 (m, 10H), δ 5.50 (s, 2H), 4.34-4.20 (m, 14H), 2.64-2.60 (t, 10H, $J = 6.94$ Hz), 1.96-1.87 (m, 14H), 1.62-1.57 (m, 22H), 1.41-1.32 (m, 50H), 0.94-0.86 (m, 30H).

^{13}C NMR (100 MHz, $CDCl_3$, δ in ppm): δ 149.45, 149.27, 148.97, 148.86, 148.36, 147.87, 146.85, 144.16, 144.09, 144.03, 131.90, 131.78, 131.71, 128.88, 128.66, 124.28, 123.64, 123.57, 122.71, 121.36, 120.66, 120.58, 120.17, 107.62, 107.24, 99.66, 99.47, 98.90, 97.43, 87.19, 84.23, 74.84, 70.19, 70.03, 69.85, 69.71, 69.65, 69.55, 69.35, 64.19, 50.59, 36.10, 32.08,

31.84, 31.62, 31.11, 30.69, 30.44, 29.85, 29.59, 29.48, 29.10, 26.65, 26.45, 26.00, 22.82, 22.68, 14.21, 14.19.

HRMS (MALDI) for $C_{132}H_{169}N_3O_7$ (M + H): calculated – 1910.3072; found- 1910.3203.

Compound 9a:

FT-IR (cm^{-1}): 2959.10, 2929.57, 2857.79, 2210.30, 1733.90, 1616.13, 1512.99, 1468.40, 1434.70, 1379.93, 1262.38, 1170.52, 1085.90, 1042.84, 838.28, 802.90, 732.25, 595.03, 555.83.

1H NMR (400 MHz, $CDCl_3$, δ in ppm): δ 7.82-7.81 (m, 6H), δ 7.55-7.47 (m, 10H), δ 7.23 (s, 1H), δ 7.18-7.15 (m, 10H), δ 4.28-4.17 (m, 16H), δ 3.05-3.01 (t, 2H, $J = 7.40$ Hz), δ 2.62-2.61 (m, 10H), 2.34-2.31 (t, 2H, $J = 6.68$ Hz), 1.92-1.83 (t, 10H, $J = 7.16$ Hz), 1.81-1.79 (m, 4H), 1.63-1.57 (m, 22H), 1.39-1.33 (m, 42H), 0.92-0.87 (m, 30H).

^{13}C NMR (100 MHz, $CDCl_3$, δ in ppm): δ 149.14, 146.71, 144.15, 131.90, 131.78, 131.65, 128.72, 128.68, 123.84, 120.53, 107.26, 106.78, 99.41, 69.81, 36.12, 31.85, 31.62, 31.09, 29.58, 26.00, 22.81, 22.68, 14.22, 14.19.

HRMS (MALDI) for $C_{130}H_{165}N_3O_7$ (M + H): calculated – 1882.2759; found- 1882.2706.

Compound 9b:

FT-IR (cm^{-1}): 2959.70, 2928.25, 2856.63, 2210.10, 1737.80, 1616.08, 1512.89, 1468.40, 1434.49, 1379.43, 1262.10, 1170.45, 1085.90, 1042.32, 838.32, 802.90, 726.71, 597.89, 558.85.

1H NMR (400 MHz, $CDCl_3$, δ in ppm): δ 7.83-7.81 (m, 6H), δ 7.54-7.48 (m, 10H), δ 7.27 (s, 1H), δ 7.17-7.68 (m, 10H), δ 4.35-4.32 (t, 2H, $J = 6.12$ Hz), δ 4.28-4.20 (m, 14H), δ 3.05-3.01 (t, 2H, $J = 7.16$ Hz), δ 2.66-2.62 (m, 10H), 2.34-2.31 (t, 2H, $J = 7.06$ Hz), 1.95-1.87 (m, 12H), 1.80-1.77 (m, 2H), 1.61-1.57 (m, 22H), 1.38-1.28 (m, 46H), 0.92-0.89 (m, 30H).

^{13}C NMR (100 MHz, $CDCl_3$, δ in ppm): δ 160.25, 148.97, 147.41, 144.18, 131.89, 131.77, 131.69, 128.91, 128.68, 123.68, 120.99, 120.55, 120.15, 107.53, 107.26, 99.70, 87.17, 84.21, 69.78, 50.32, 36.12, 31.84, 31.62, 31.12, 31.09, 30.60, 29.85, 29.57, 29.24, 29.08, 26.63, 26.33, 26.01, 22.82, 22.68, 14.22, 14.20.

HRMS (MALDI) for $C_{132}H_{169}N_3O_7$ (M + H): calculated – 1910.3072; found- 1910.3152.

Compound 9c:

FT-IR (cm⁻¹): 2959.70, 2928.61, 2856.84, 2210.10, 1741.70, 1616.08, 1512.89, 1468.40, 1434.65, 1379.77, 1262.10, 1170.59, 1085.90, 1041.72, 839.92, 802.90, 730.61, 597.89, 547.14.

¹H NMR (400 MHz, CDCl₃, δ in ppm): δ 7.83-7.81 (m, 6H), δ 7.54-7.49 (m, 10H), δ 7.29 (s, 1H), δ 7.17-7.16 (m, 10H), δ 4.36-4.33 (t, 2H, *J* = 6.14 Hz), δ 4.27-4.21 (m, 14H), δ 3.05-3.01 (t, 2H, *J* = 7.28 Hz), δ 2.64-2.61 (t, 10H, *J* = 7.10 Hz), 2.34-2.31 (t, 2H, *J* = 6.68 Hz), 1.95-1.82 (m, 14H), 1.65-1.57 (m, 22H), 1.39-1.22 (m, 50H), 0.95-0.90 (m, 30H).

¹³C NMR (100 MHz, CDCl₃, δ in ppm): δ 149.33, 149.15, 148.74, 147.75, 144.03, 143.90, 131.77, 131.65, 131.59, 128.76, 128.54, 124.16, 123.52, 122.58, 120.54, 120.46, 120.04, 107.49, 107.16, 107.11, 99.54, 99.34, 98.78, 97.31, 87.07, 84.10, 74.71, 69.91, 69.58, 69.43, 69.23, 64.07, 50.46, 35.98, 31.95, 31.72, 31.49, 30.98, 30.57, 30.31, 29.73, 29.46, 29.35, 28.98, 26.53, 26.33, 25.88, 14.09, 14.06.

HRMS (MALDI) for C₁₃₄H₁₇₃N₃O₇ (M + H): calculated – 1938.3385; found- 1938.3344.

3. NMR spectral data (¹H and ¹³C NMR)

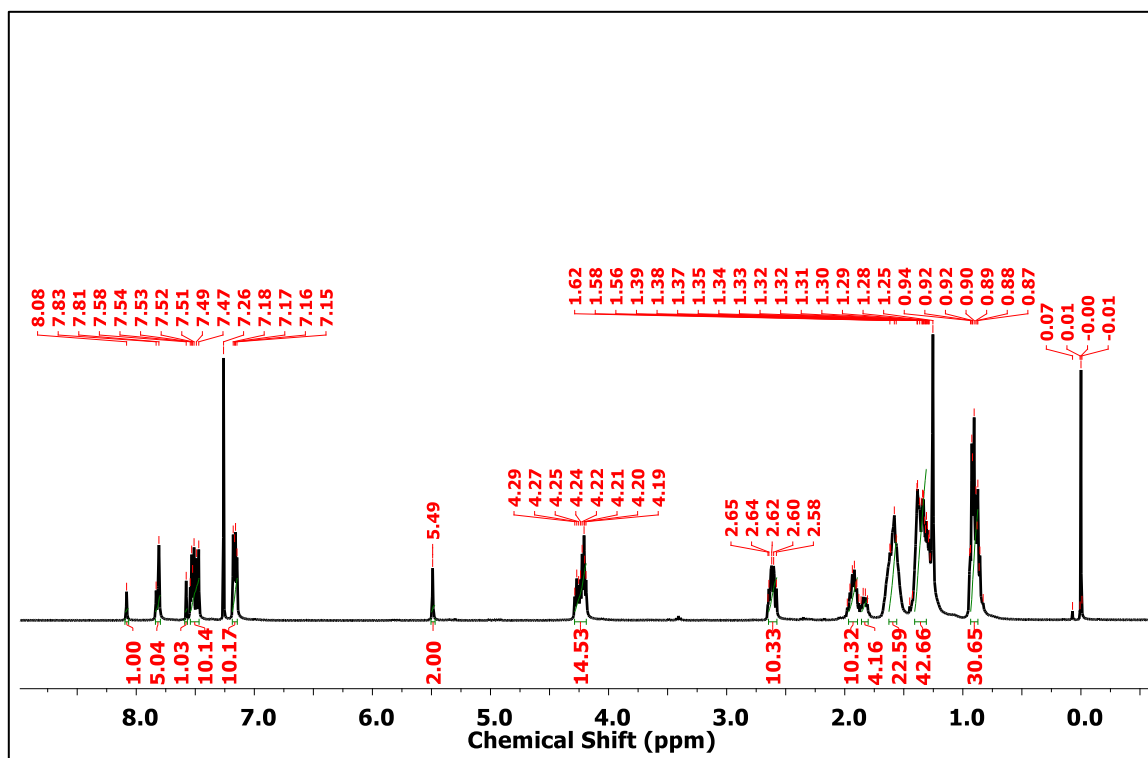


Fig. S1 ¹H NMR spectra of compound 8a.

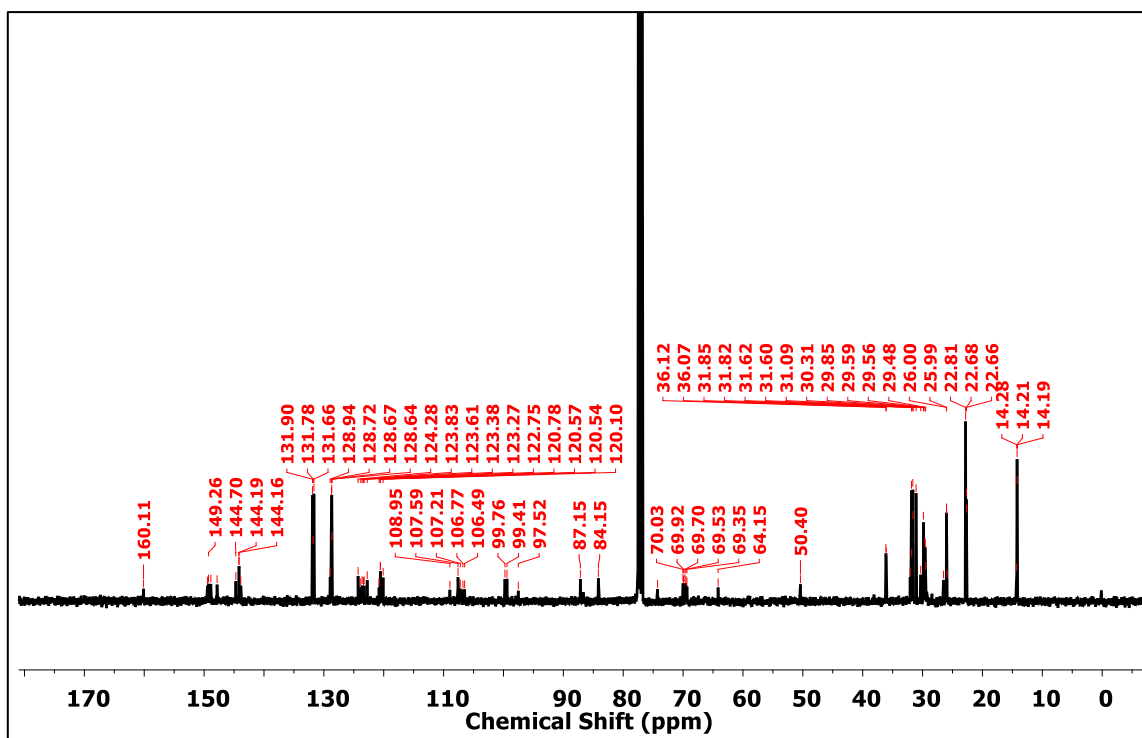


Fig. S2 ^{13}C NMR spectra of compound **8a**.

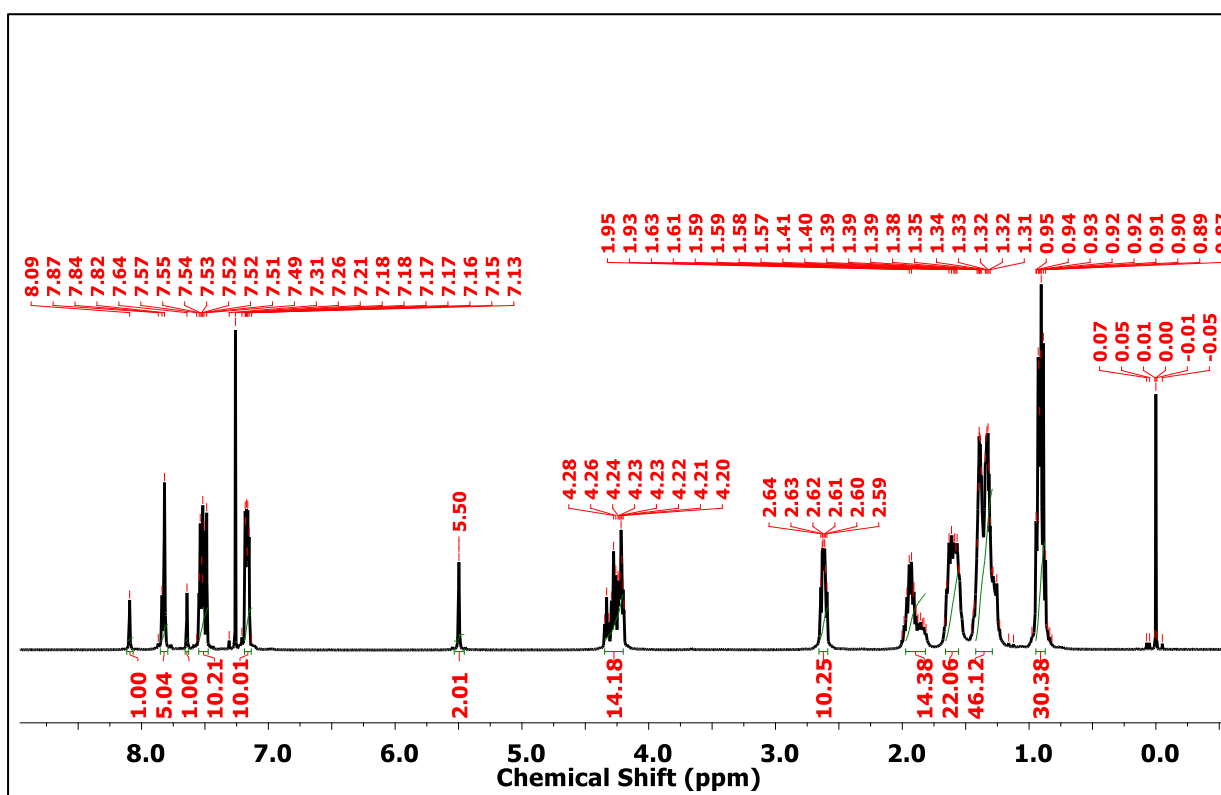


Fig. S3 ^1H NMR spectra of compound **8b**.

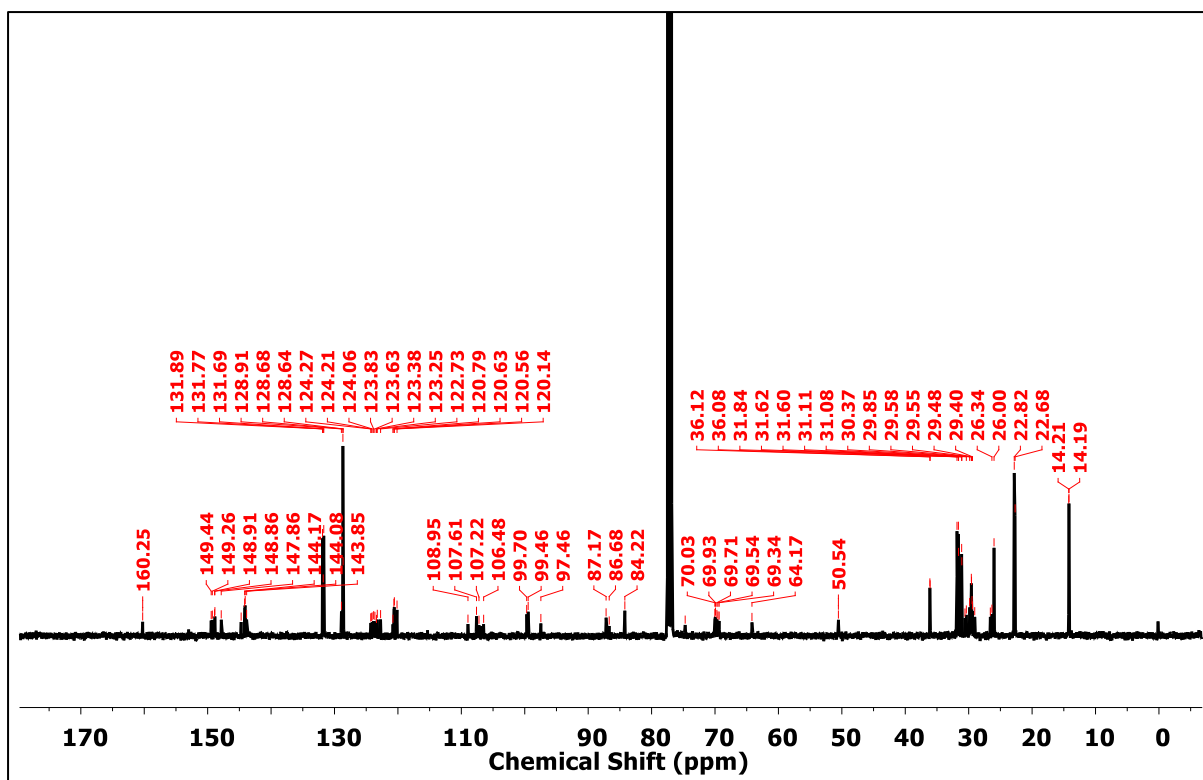


Fig. S4 ^{13}C NMR spectra of compound **8b**.

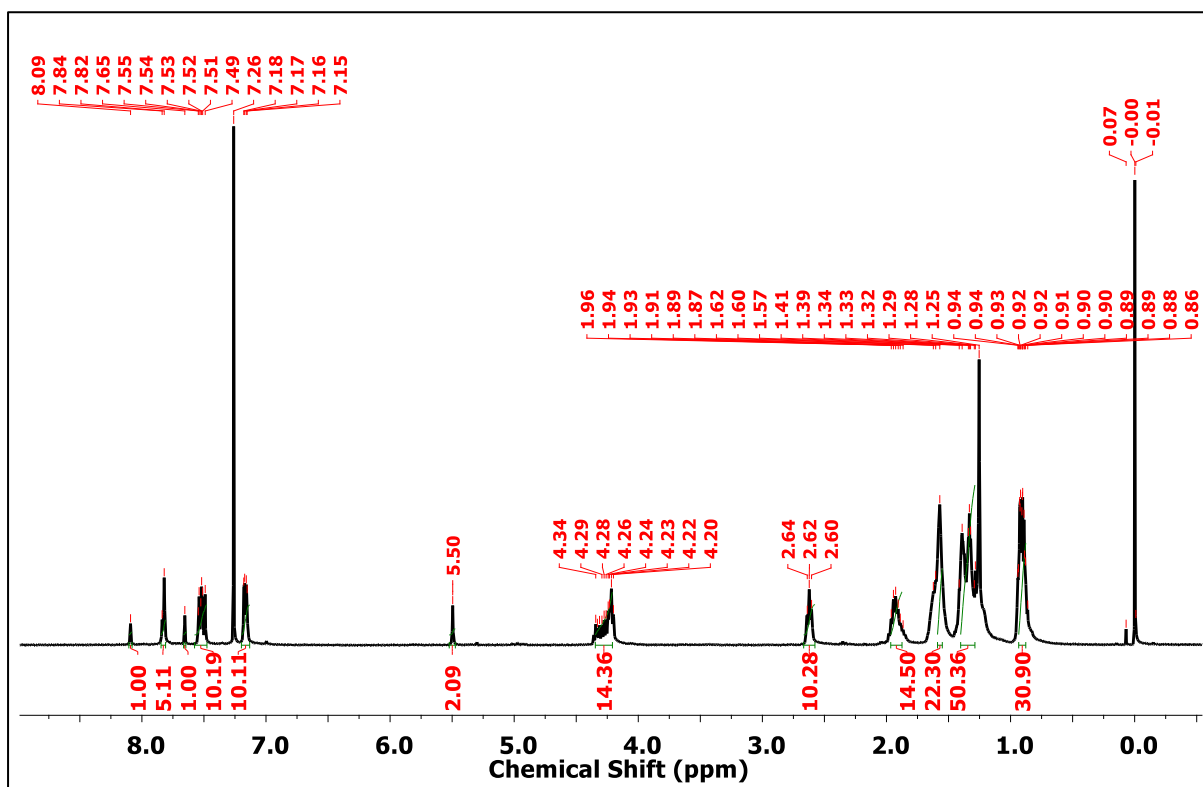


Fig. S5 ^1H NMR spectra of compound **8c**.

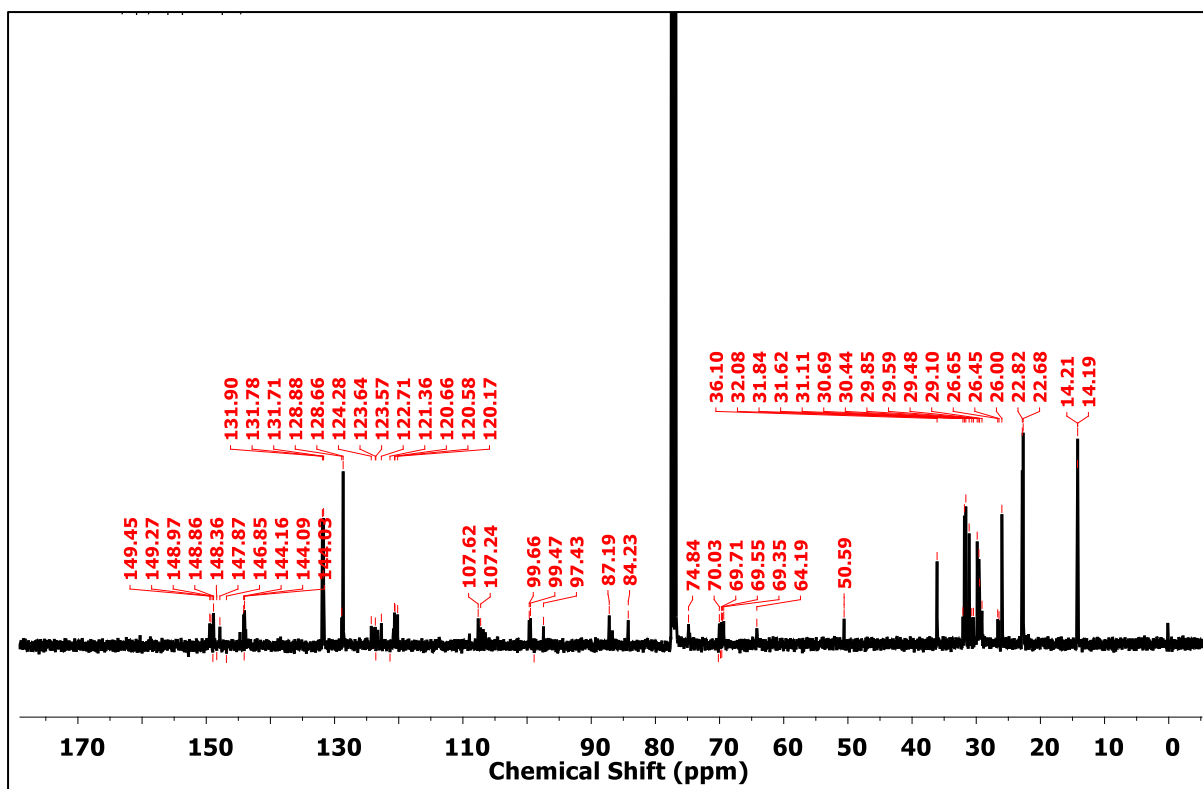


Fig. S6 ^{13}C NMR spectra of compound **8c**.

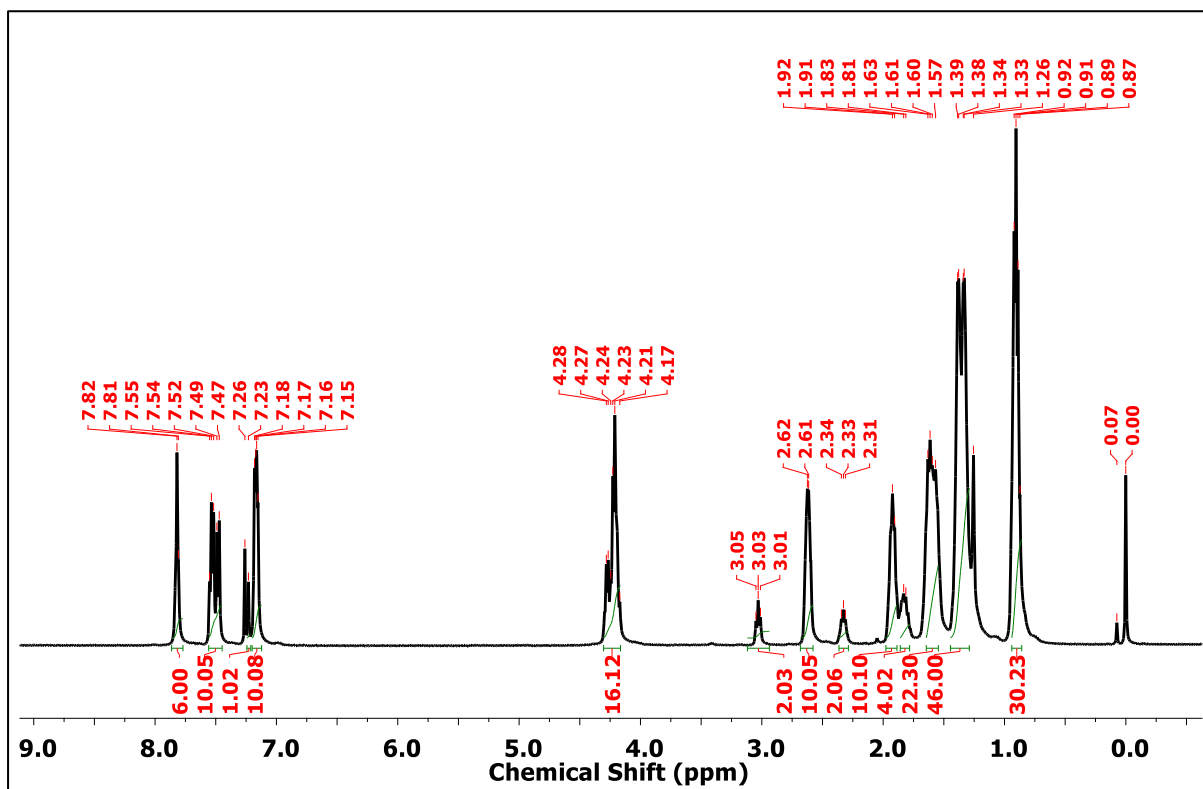


Fig. S7 ^1H NMR spectra of compound **9a**.

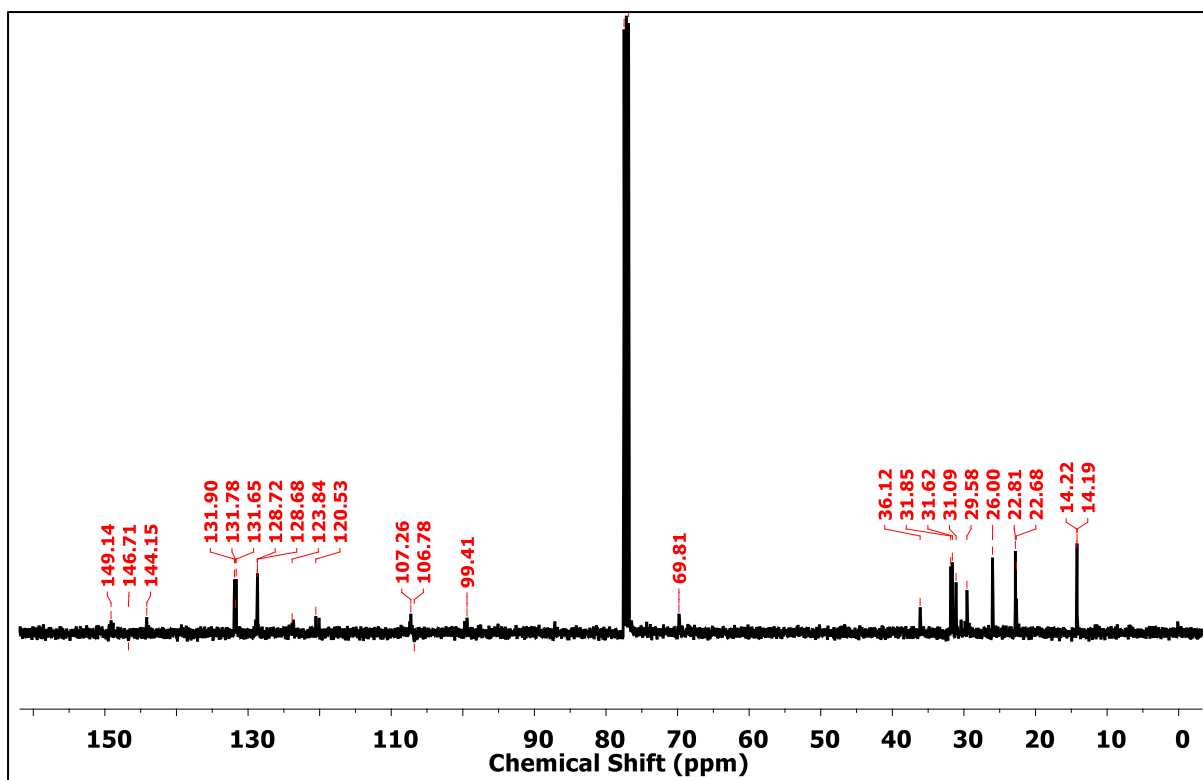


Fig. S8 ¹³C NMR spectra of compound **9a**.

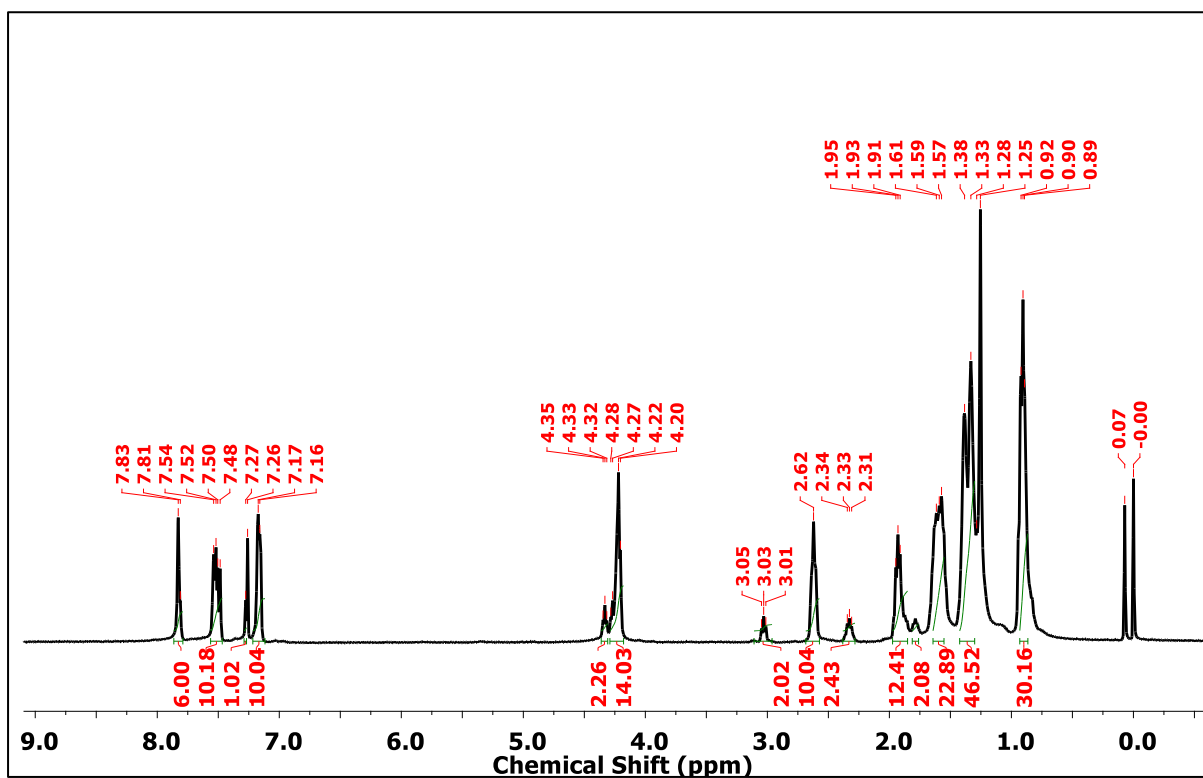


Fig. S9 ¹H NMR spectra of compound **9b**.

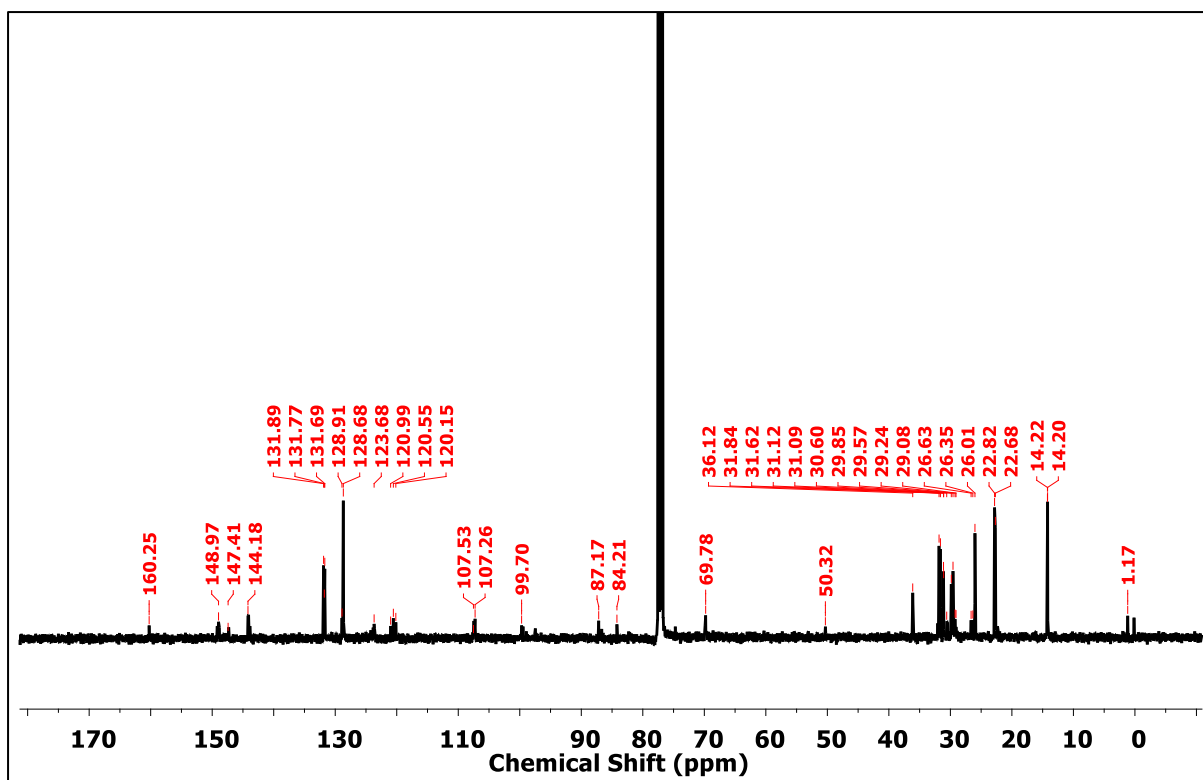


Fig. S10 ^{13}C NMR spectra of compound 9b.

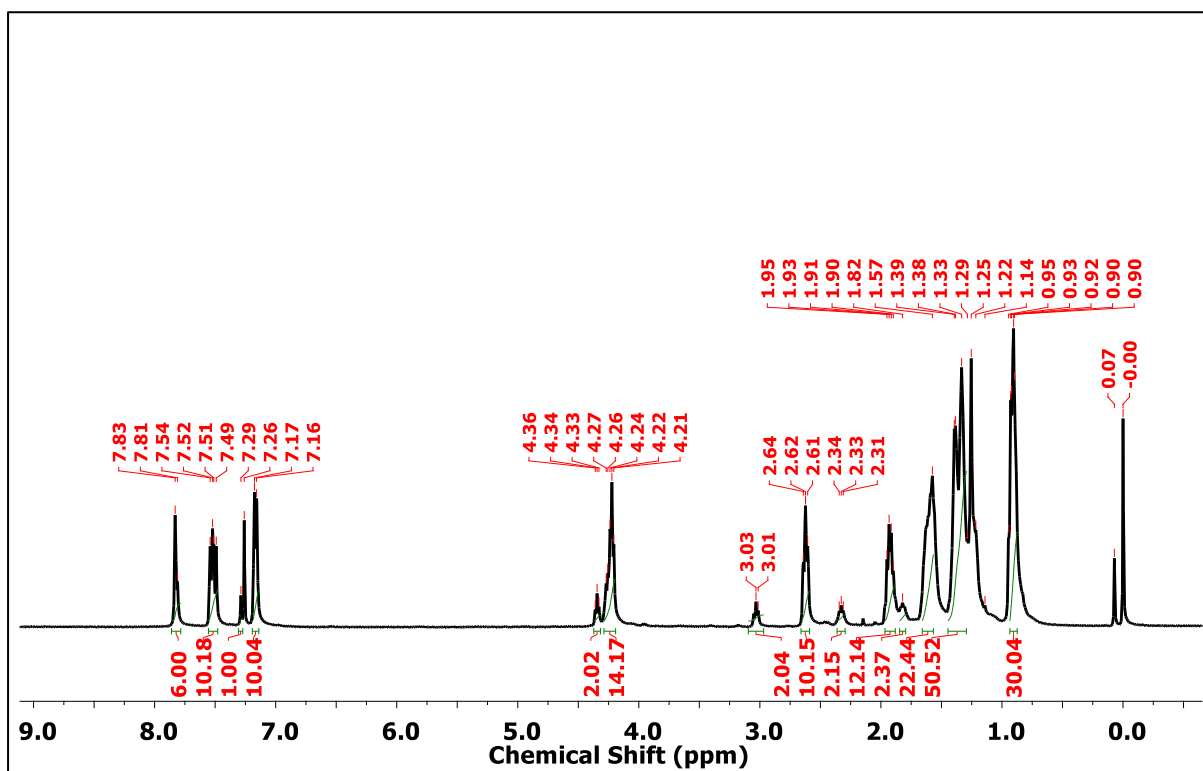


Fig. S11 ^1H NMR spectra of compound 9c.

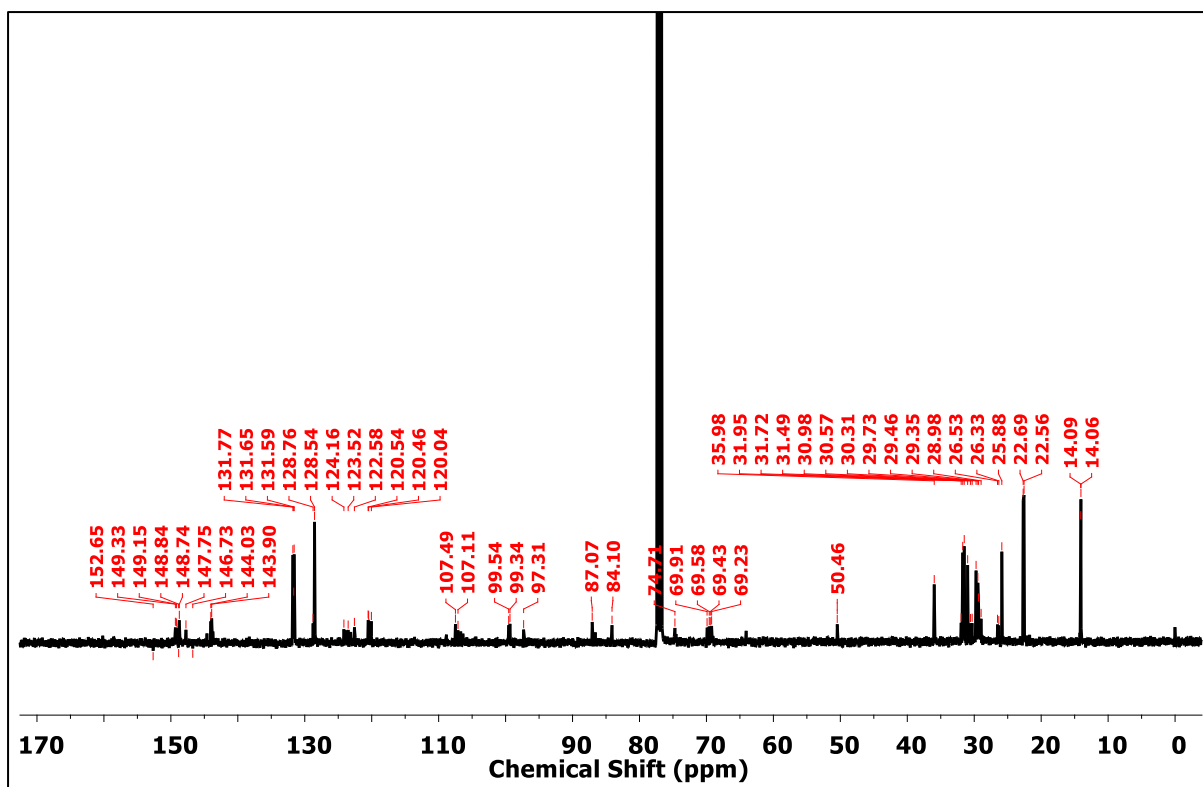


Fig. S12 ^{13}C NMR spectra of compound **9c**.

4. FT-IR spectral data

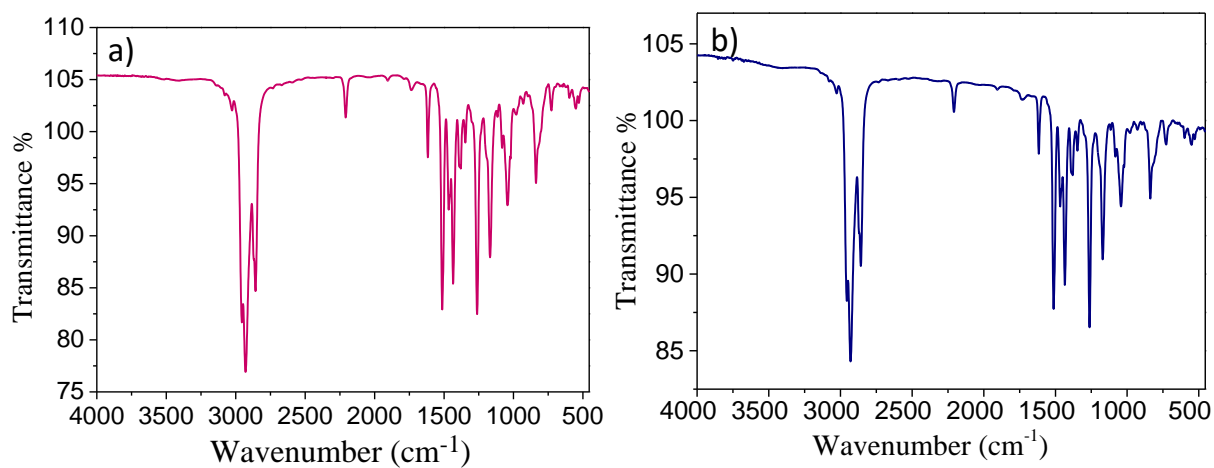


Fig. S13 FT-IR spectra of compound **8a** and **9a**, respectively.

5. DSC Thermograms

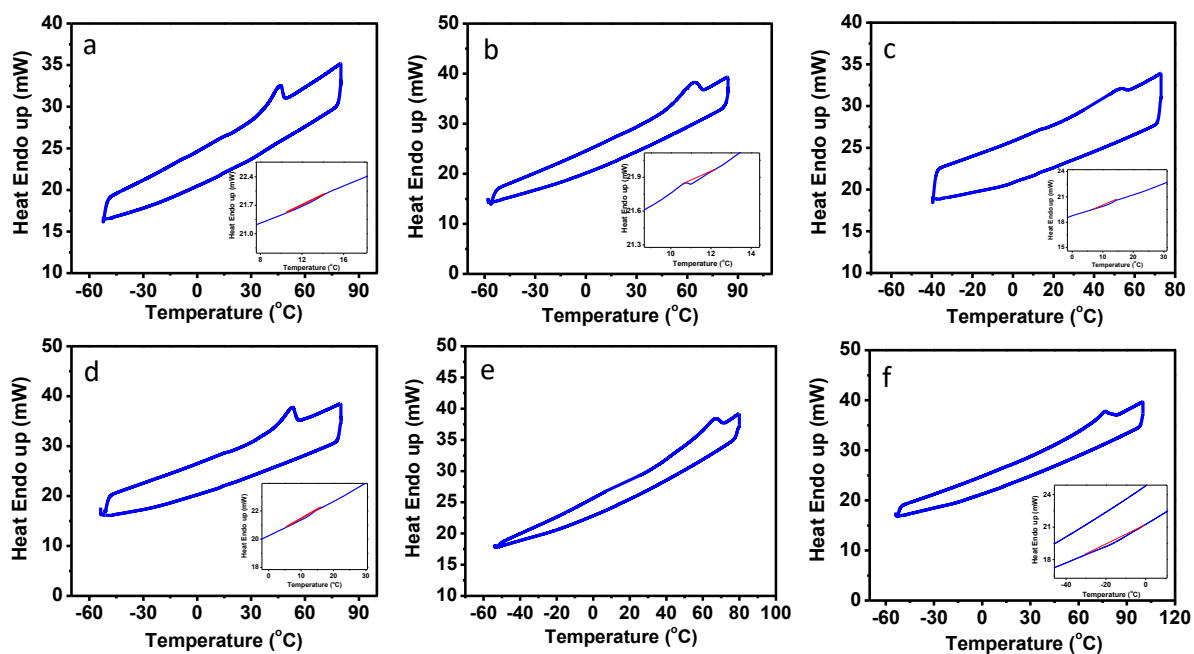


Fig. S14. DSC thermogram for the pure series of compound: (a) **8a**; (b) **8b**; (c) **8c**; (d) **9a**; (e) **9b**; (f) **9c**, recorded with the scan rate of 10 °C/ min.

6. X-ray data

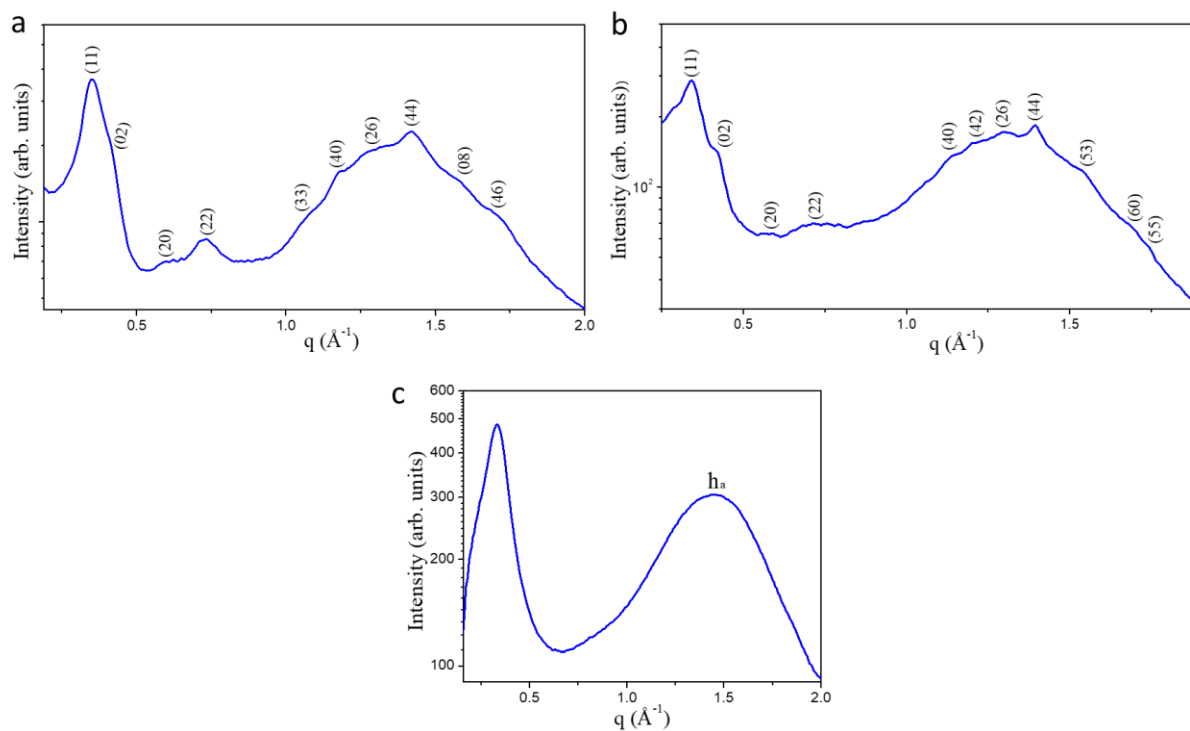


Fig. S15 X-Ray diffraction pattern for the pure compounds: (a) Col_r phase at 25 °C for **8a**; (b) Col_r phase at 25 °C for **8b**; (c) weak smectic phase at 25 °C for **8c**.

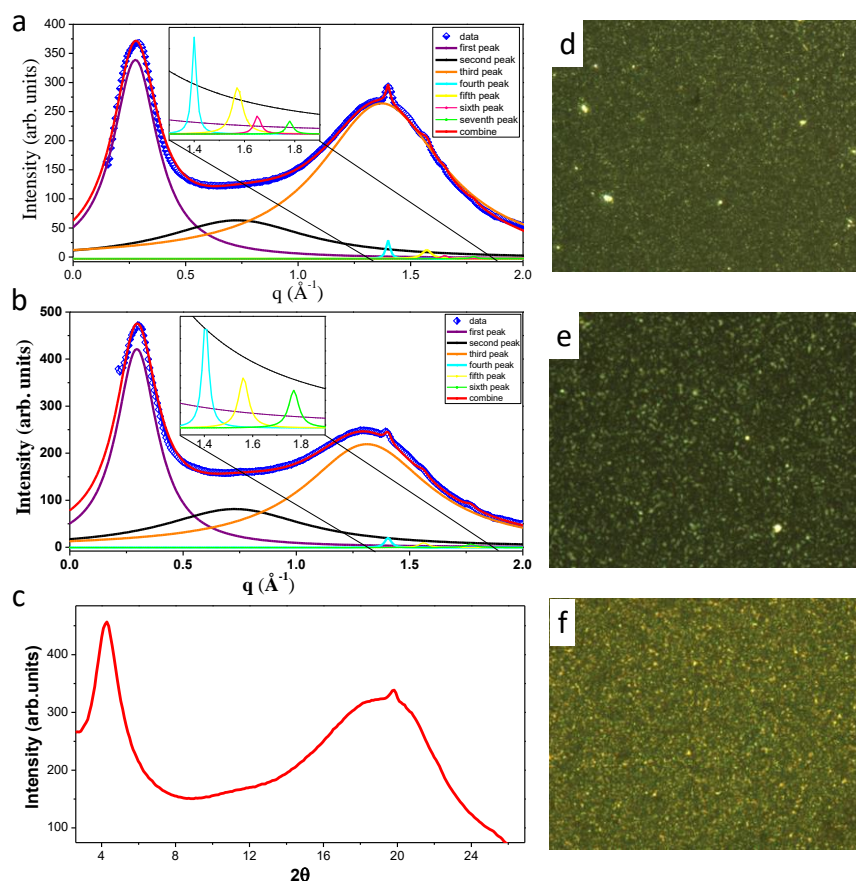


Fig. S16 X-Ray diffraction pattern for the pure compounds: (a) N_C phase at 10.0 °C for **8a**; (b) N_C phase at 5.0 °C for **9a**; (c) smectic phase at -20.0 °C for **9c**; POM textures on upon cooling: (d) for **8a** at 10.4 °C; (e) for **9a** at 5.8 °C; (f) for **9c** at -20.0 °C, recorded with the rate of 10 °C/min.

For compound **8a** at 10.0 °C (Fig. S16a): The first peak in color purple with spacing 22.77 Å is due to average column-column separation. The second peak in black color is mainly due to background and it is not our concern. The third peak in orange color with spacing 4.60 Å, appearing mainly due to fluid alkyl chain to chain correlation. However, the fourth peak in cyan color with spacing 4.40 Å correlates the average partial chain to chain spacing. Interestingly, the seventh peak in color green with spacing 3.53 Å attributing the disc to disc separation in column indicating the occurrence of columnar nematic (N_C) phase. Further, the fifth (in color yellow) and sixth (in color cyan) peaks with spacing 3.99 Å & 3.80 Å appearing most possibly due to other kind of arrangement of alkyl chains. Red color curve represents the combine results of all peaks and well fitted to experimental X-Ray diffraction data. The similar behaviour of diffractogram has been observed in case of **8b**.

For compound **9a** at 5.0 °C (Fig. S16b): The first peak in color purple with spacing 21.23 Å is due to average column-column separation. The second peak in black color is mainly due to background and it is not our concern. The third peak in orange color with spacing 4.78 Å, appearing mainly due to fluid alkyl chain to chain correlation. However, the fourth peak in cyan color with spacing 4.42 Å correlates the average partial chain to chain spacing. Interestingly, the sixth peak in color green with spacing 3.55 Å attributing the disc to disc separation in column suggesting the formation of columnar nematic (N_C) phase. Further, the fifth in color yellow peak with spacing 4.01 Å appearing most possibly due to different kind of arrangement of alky chains. Red color curve represents the combine results of all peaks and well fitted to experimental X-Ray diffraction data. The similar behaviour of diffractogram has been observed in case of **9b**.

For **9c** at -20.0 °C (Fig. S16c): The first peak at 20.09 Å was observed in a similar manner to its diffractogram at room temperature. The additional peak at 4.43 Å correlates the average partial chain to chain spacing. There was no core to core peak appears in the wide angle region which excludes the possibility of N_C phase. The similar behaviour of diffractogram has been observed in case of **8c**.

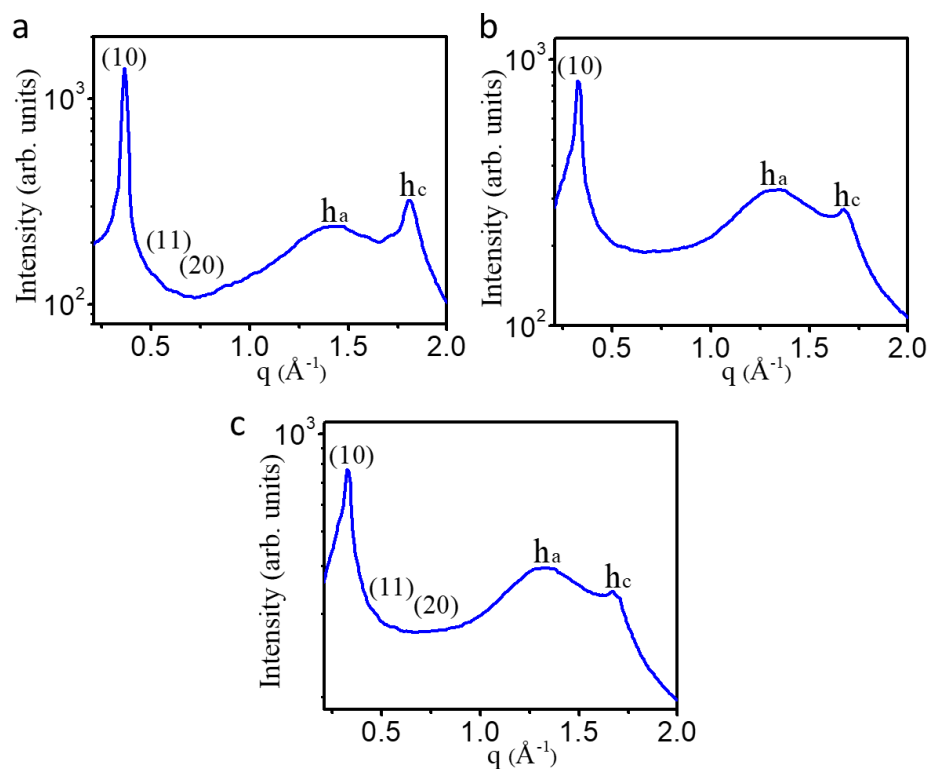


Fig. S17 X-Ray diffraction pattern for 2:1 ratio of TNF: compound complex: (a) Col_h phase at 25 °C for **8a**/TNF complex; (b) Col_h phase at 25 °C for **8b**/TNF complex; (c) Col_h phase at 25 °C **8c**/TNF complex.

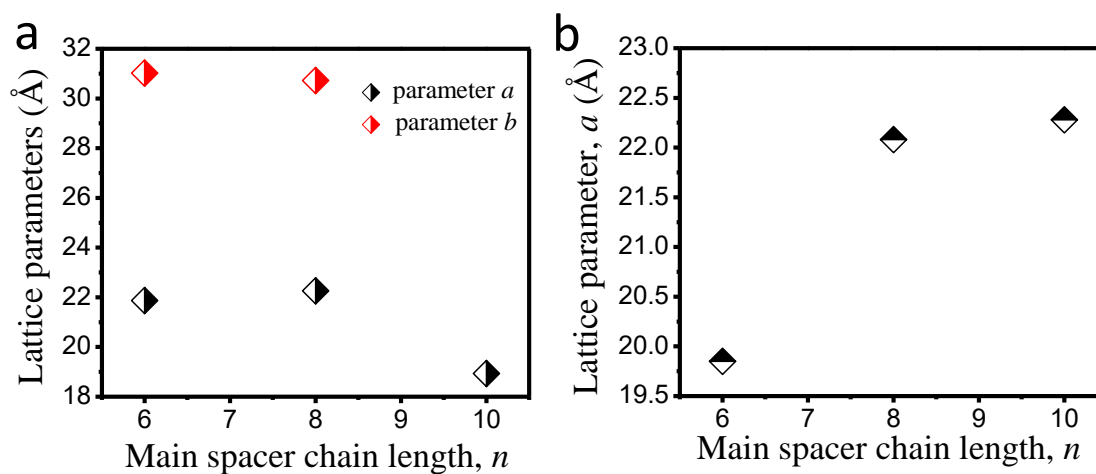


Fig. S18 Variation of lattice parameter for (a) pure compound **8a**, **8b** and **8c**; (b) 2:1 TNF/compound complex: **8a**/TNF, **8b**/TNF and **8c**/TNF.

Table S1. The Indices observed and calculated *d*-spacings and planes of the diffraction peaks for the 2D columnar centered rectangular (Col_r) phase observed for the pure compound of series of compound **8**.

compound	(hk)	d-spacing Experimental d_{obs} (Å)	d-spacing Calculated d_{cal} (Å)	Lattice parameter, (Å)	Phase
8a	11	17.88	17.87	$a = 21.87$ $b = 31.02$	Columnar rectangular
	02	15.51	15.51		
	20	10.65	10.94		
	22	8.73	8.94		
	33	5.95	5.96		
	40	5.33	5.47		
	26	4.83	4.67		
	44	4.43	4.47		
	08	3.97	3.88		
	46	3.69	3.76	h_c	
8b	11	18.21	18.03	$a = 22.26$ $b = 30.72$	Columnar rectangular
	02	15.36	15.36		
	20	11.14	11.13		
	22	8.82	9.01		
	40	5.52	5.57		
	42	5.21	5.23		
	26	4.82	4.65		
	44	4.50	4.51		
	53	4.10	4.08		
	60	3.71	3.71		
	55	3.6	3.60	h_c	
8c		18.93	-	22.28	Disordered Smectic
		4.34		h_a	

Table S2. The Indices observed and calculated d -spacings and planes of the diffraction peaks for the columnar hexagonal (Col_h) phase observed for 2:1 TNF/compound complex for series of compound **8**.

Complex	(hk)	d-spacing Experimental d_{obs} (Å)	d-spacing Calculated d_{cal} (Å)	Lattice parameter, a (Å)	Phase
8a /TNF	(10)	17.19	17.19	19.85	Columnar hexagonal
	h_a	4.42			
	h_c	3.48			
8b /TNF	(10)	19.12	19.12	22.08	Columnar hexagonal
	h_a	4.74			
	h_c	3.74			
8c /TNF	(10)	19.30	19.66	22.28	Columnar hexagonal
	(11)	11.10			
	h_a	4.74			
	h_c	3.73			

7. Absorption and Emission studies

7.1 Absorption and emission studies in solution state:

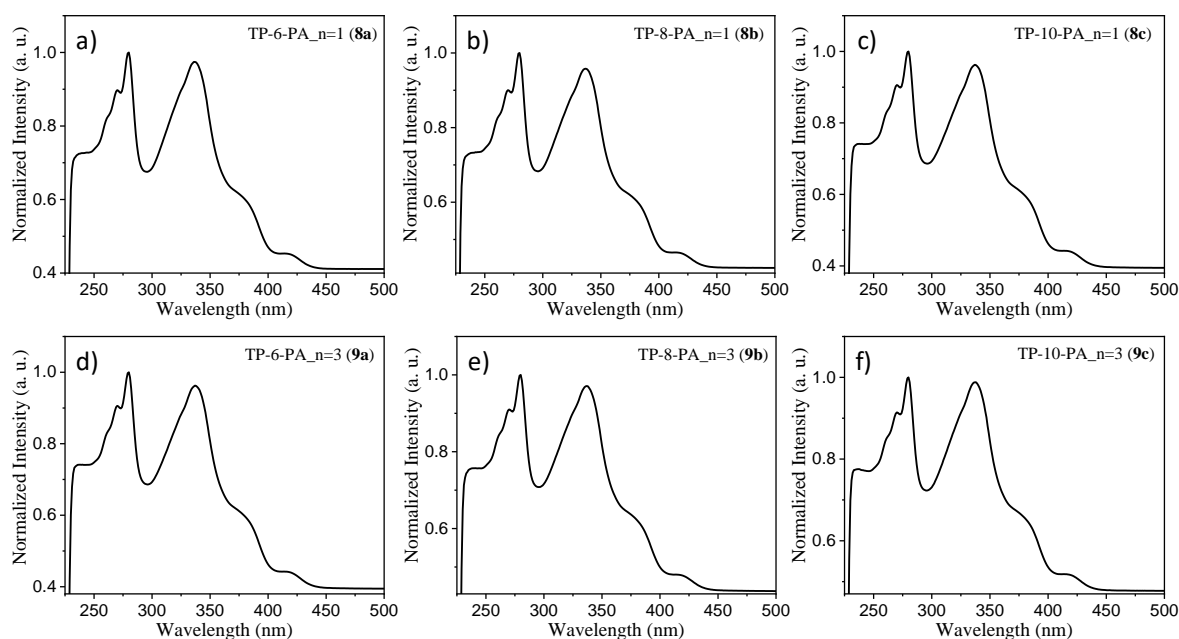


Fig. S19 Absorption spectra of compound **8a** (a); **8b** (b); **8c** (c) **9a** (d); **9b** (e); **9c** (f) in CHCl₃ solution.

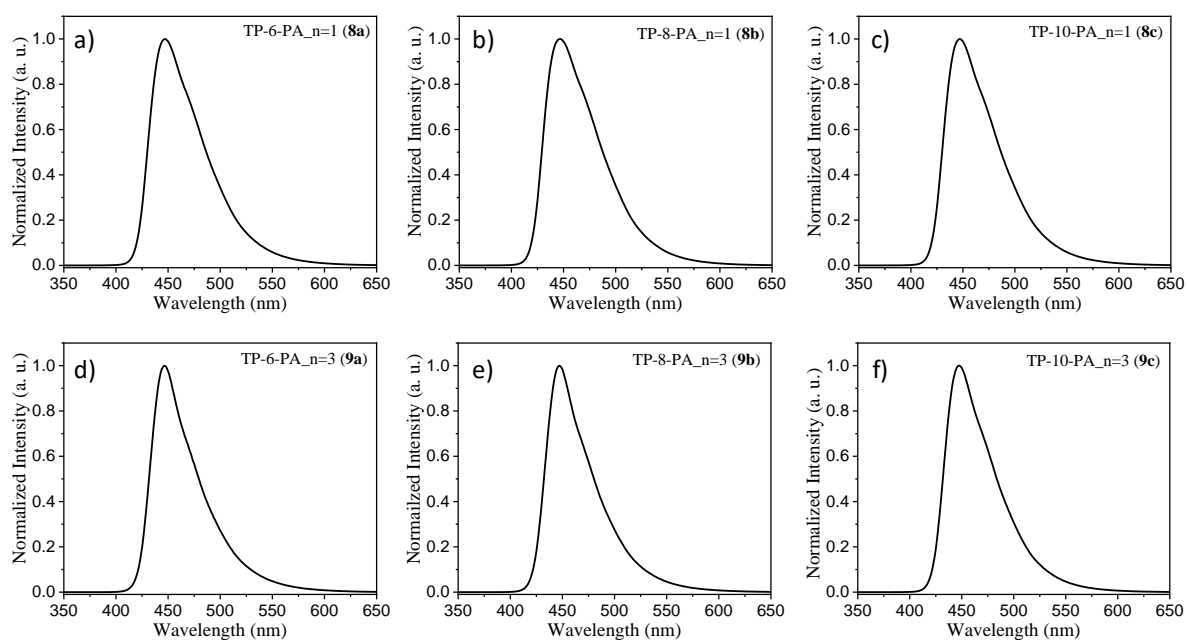


Fig. S20 Emission spectra of compound **8a** (a); **8b** (b); **8c** (c) **9a** (d); **9b** (e); **9c** (f) in CHCl_3 solution.

7.2 Absorption and emission studies in solid state:

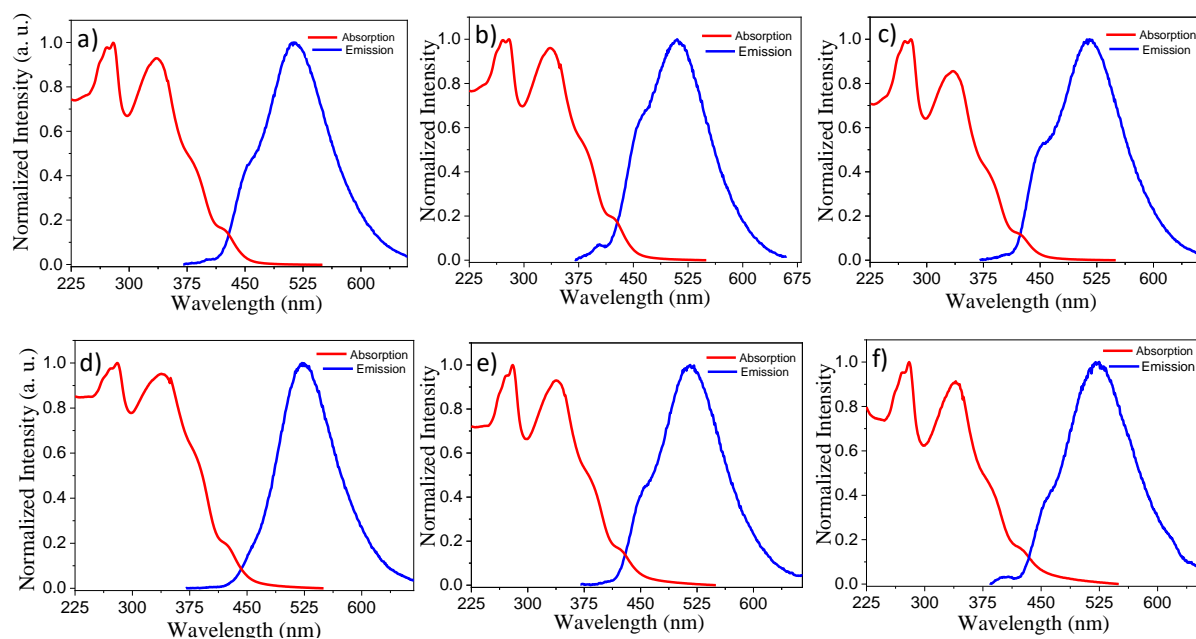


Fig. S21 Emission spectra of compound **8a** (a); **8b** (b); **8c** (c) **9a** (d); **9b** (e); **9c** (f) in thin film state.

8. Quantum yield Calculation (Relative)¹

The details are reported elsewhere¹. Briefly, the calculation details are below and reproduced as mentioned in our earlier manuscript.¹

“Relative quantum yield was obtained according to well-known procedure by using quinine sulphate in 0.1 M H₂SO₄ solution as the standard. Quantum yield values were calculated according to the following equation:

$$Q_S = Q_R \times (m_S/m_R) \times (n_S/n_R)^2,$$

Where Q: Quantum yield, m: slope of the plot of integrated fluorescence intensity vs absorbance, n = refractive index (1.445 for CHCl₃ and 1.33 for distilled water).

Subscript R refers to the reference fluorophore i.e quinine sulphate in 0.1 M H₂SO₄ and subscript S refers to the sample under investigation. In order to minimise the re-absorption effects, absorbance value was kept below 0.15 at the excitation wavelength of 337 nm.

Quantum yield of quinine sulphate in 0.1M H₂SO₄ solution is 0.54. After substituting the appropriate values, the simplified equation is:

$$\begin{aligned} Q_S &= 0.54 \times (m_S/m_R) \times (1.445/1.33)^2 \\ &= 0.5867 \times (m_S/m_R)'' \end{aligned}$$

Table S3 Quantum yield values of compound **5**

Entry	m _S	m _R	Q _S ^{a,b,c}
8a	10.957 x 10 ⁷	13.937 x 10 ⁷	0.461
8b	11.198 x 10 ⁷	13.937 x 10 ⁷	0.471
8c	10.358 x 10 ⁷	13.937 x 10 ⁷	0.436
9a	8.261 x 10 ⁷	13.937 x 10 ⁷	0.348
9b	9.846 x 10 ⁷	13.937 x 10 ⁷	0.414
9c	10.125 x 10 ⁷	13.937 x 10 ⁷	0.426

^aMeasured in CHCl_3 .

^bExcited at absorption maxima.

^cStandard Quinine sulphate ($Q_f = 0.54$) in 0.1 M H_2SO_4 .

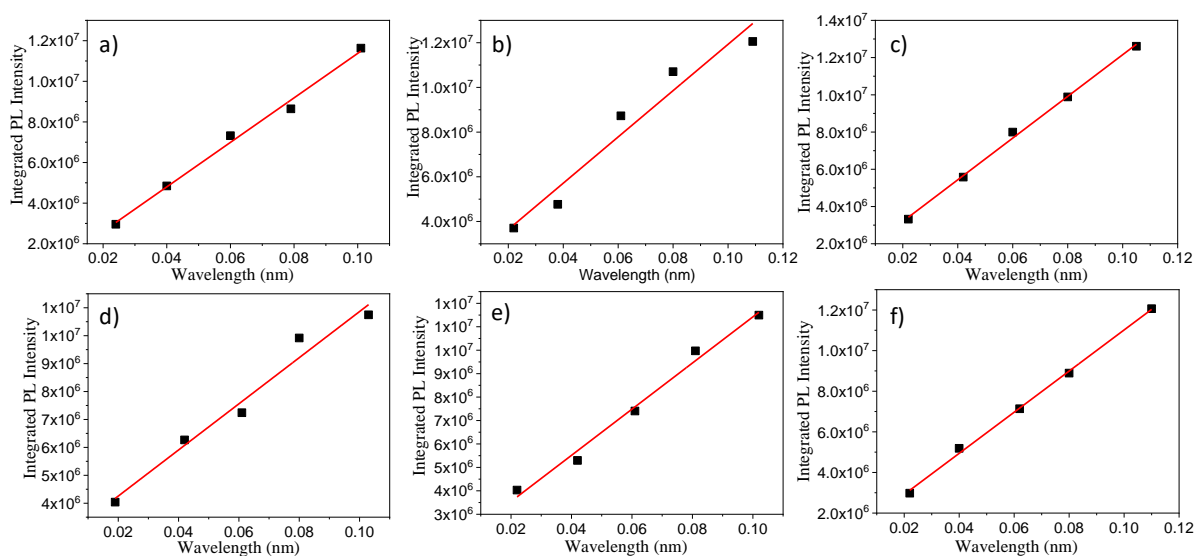


Fig. S22 Plots of integrated photoluminescence intensity vs absorbance of compounds **8a** (a); **8b** (b); **8c** (c); **9a** (d); **9b** (e); **9c** (f) measured in HPLC chloroform excited at 337 nm.

9. Fluorescence decay measurements

The decay curves were bi-exponential and analysed by using standard method of non-linear least square fitting method. The quality of fits was judged using statistical parameters, reduced χ^2 value and the residual data.

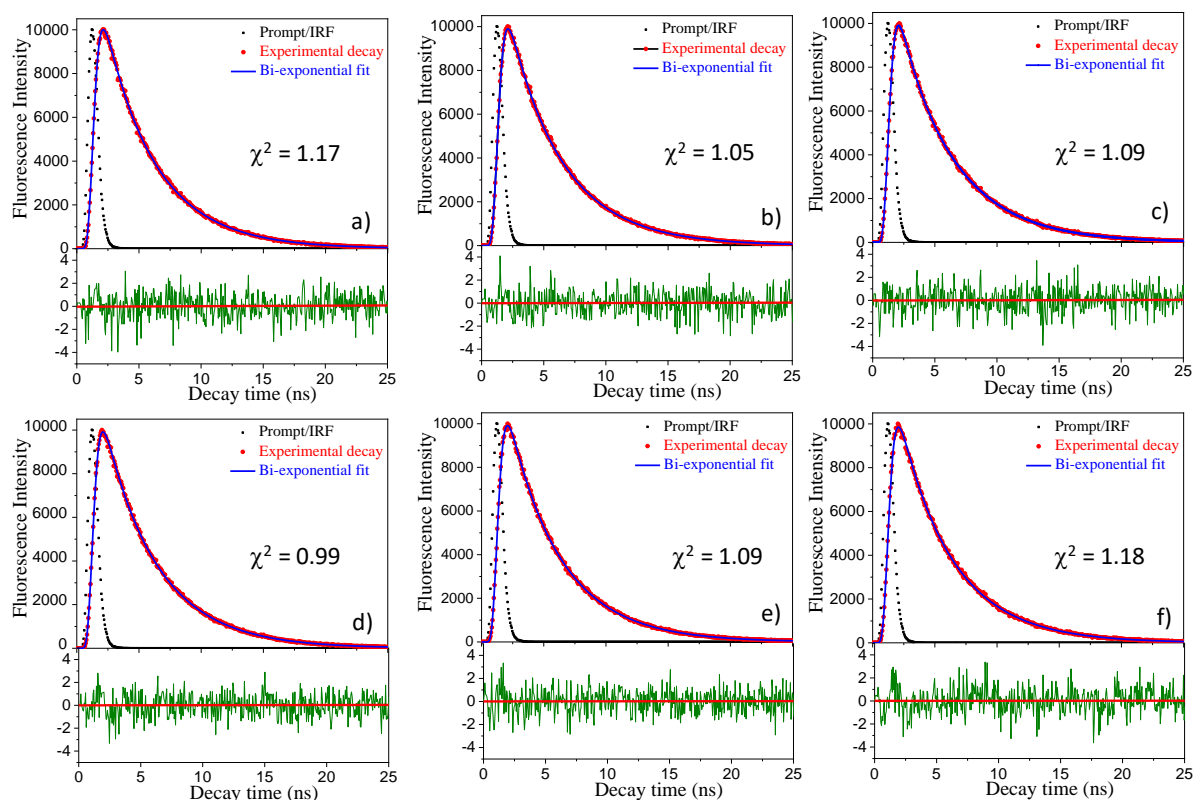


Fig. S23 Fluorescence decay spectra of compounds (a) **8a**; (b) **8b**; (c) **8c**; (d) **9a**; (e) **9b**; (f) **9c**; for $\lambda_{\text{exc}} = 337$ nm & $\lambda_{\text{ems}} = 447$ nm in micromolar chloroform solution.

10. References

1. I. Bala, S. P. Gupta, J. De and S. K. Pal, *Chem. – Eur. J.*, 2017, **23**, 12767.
2. M. Gupta, S. P. Gupta, M. V. Rasna, D. Adhikari, S. Dhara and S. K. Pal, *Chem. Commun.*, 2017, **53**, 3014.
3. Y. F. Bai, K. Q. Zhao, P. Hu, B. Q. Wang and C. Redshaw, *Curr. Org. Chem.*, 2013, **17**, 871.
4. S. K. Gupta, V. K. Raghunathan, V. Lakshminarayanan, S. J. Kumar, *J. Phys. Chem. B*, 2009, **113**, 12887.
5. M. Gupta, I. Bala and S. K. Pal, *Tetrahedron Lett.*, 2014, **55**, 5836.